tvst

Public Health

Visual Deficits in Type 2 Diabetes Mellitus Without Retinopathy: From Retinal Structure to Higher-Level Visual Functions

Sha Luo[1], Lin Xia[1], Yue Wang[1], Yong Tang[2], Jiong Dong[1], Rong Liu[3], and Lixia Feng[1]

[1] Department of Ophthalmology, First Affiliated Hospital of Anhui Medical University, Hefei, People's Republic of China
[2] Department of Medical Technology, Anhui Medical College, Hefei, Anhui, People's Republic of China
[3] School of Life Sciences, Division of Life Sciences and Medicine, University of Science and Technology of China, Hefei, People's Republic of China

Correspondence: Lixia Feng, Department of Ophthalmology, First Affiliated Hospital of Anhui Medical University, No. 81 Meishan Rd., Hefei City, Anhui Province 230032, People's Republic of China. e-mail: lixiafeng@163.com
Rong Liu, School of Life Sciences, Division of Life Sciences and Medicine, University of Science and Technology of China, No. 96, Jin Zhai Rd., Baohe District, Hefei 230026, People's Republic of China. e-mail: rongliu@ustc.edu.cn

Received: April 2, 2024
Accepted: January 18, 2025
Published: March 11, 2025

Keywords: second-order visual function; diabetes; visual psychophysics; optical coherence tomography (OCT)

Citation: Luo S, Xia L, Wang Y, Tang Y, Dong J, Liu R, Feng L. Visual deficits in type 2 diabetes mellitus without retinopathy: From retinal structure to higher-level visual functions. Transl Vis Sci Technol. 2025;14(3):10, https://doi.org/10.1167/tvst.14.3.10

Purpose: The purpose of this study was to evaluate deficits at varying levels of visual system in diabetes without clinical retinopathy (NoDR) and to explore the optimal method for detecting early diabetic visual disorders among functional and retinal structural assessments included.

Methods: This cross-sectional study examined eyes by the Early Treatment of Diabetic Retinopathy Study (ETDRS) charts, visual psychophysical tests, optical coherence tomography (OCT), and OCT angiography (OCTA). Visual psychophysical metrics included grating acuity (GA), and contrast sensitivity to first-order motion stimuli (1stM), second-order contrast-modulated stationary stimuli (2ndS), and second-order motion stimuli (2ndM). Generalized linear mixed effect (GLME) models were applied to assess group effects and linear relationships between measurements. The receiver operating characteristic (ROC) analysis was utilized to identify the optimal classifier for detecting NoDR.

Results: Fifty-three eyes of 33 patients with NoDR and 40 eyes of 27 healthy controls were included. The NoDR group showed significant reductions in various visual functions, including ETDRS acuity, GA, 2ndS, and 2ndM (P values < 0.001), and microvascular changes in foveal vascular density (FD-300), the acircularity index (AI) of the foveal avascular zone, and the parafoveal superficial capillary plexus density (P values < 0.05). GLME models revealed these retinal variations were not significantly correlated with early diabetic visual function abnormalities. ROC analysis demonstrated the integration of GA and FD-300 (area under the curve [AUC] $= 0.911$) is the most effective classifier for detecting early diabetic visual dysfunctions.

Conclusions: In addition to retinal defects, both low- and higher-order visual function disorders along the visual pathway exist in patients with NoDR. Combining functional and structural measurements may provide more accurate assessments for detecting early diabetic visual disorders.

Translational Relevance: Sophisticated visual psychophysical measurements, including grating acuity and second-order function, could be applied for detecting early diabetic visual disorders.

Introduction

Diabetes, one of the most serious and common chronic diseases, is a leading cause of progressive vision loss.[1] Over 90% are individuals with type 2 diabetes mellitus (T2DM).[2] The neurovascular unit (NVU) was affected by diabetes mellitus, which is a functional unit consisting of neurons, blood vessels, and supporting cells in the central nervous system, leading to neural degeneration.[3,4] It is considered to be associated with the progression of diabetic

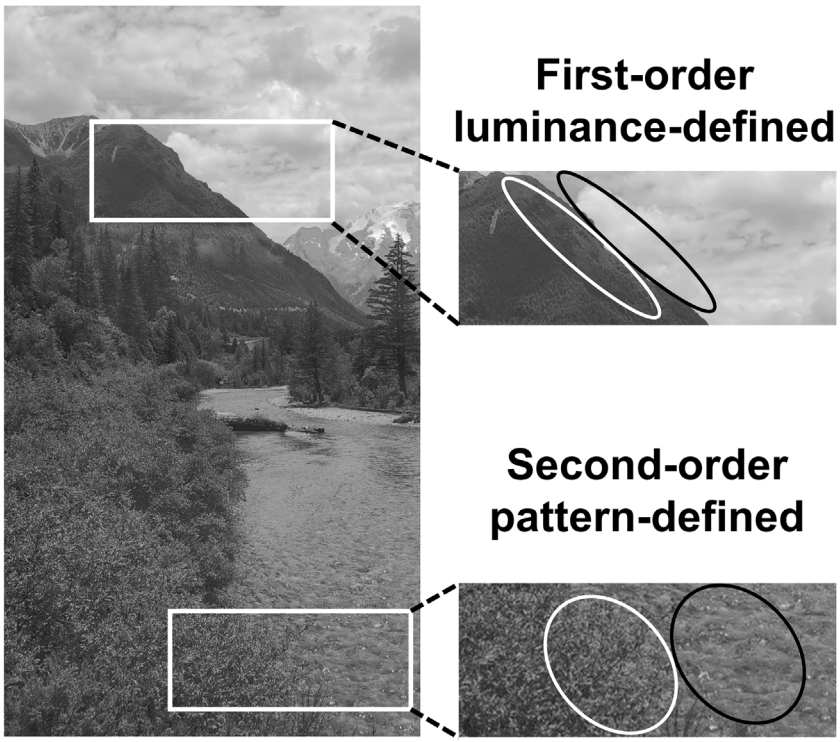

Figure 1. Illustration of first- and second-order visual information. Here, a first-order contour is defined by a luminance difference between the mountain and the cloud (first order, *top inset*). A second-order boundary is defined by a pattern difference between the bush and the river (second order, *bottom inset*).

retinopathy (DR) in the early stages of the disease. As increasing evidence of early neuronal defects prior to the onset of vascular lesions related to diabetes is found in the retina,[5–9] DR is recognized as a neurovascular complication rather than a microvascular complication of diabetes.[10] The retina has the same embryological origin and similar anatomic and physiological characteristics as the brain, so neurovascular abnormalities leading to vision loss in patients with diabetes are likely to occur in both the retina and the brain. Visual functional measurements, which reflect composite deficits along the visual pathway rather than just retinal abnormalities, can permit the identification of neurovascular damage in a subclinical stage before the recognition of DR signs. For example, visual acuity,[11] contrast sensitivity,[12,13] visual field sensitivity,[14–16] color perception,[17–20] and orientation discrimination[21] exhibit deficits even before DR. In these functional tests, the luminance-defined stimuli (first-order stimuli, such as gratings or letters) or color-defined stimuli mainly assess the visual processing at the level of the retina and primary visual cortex (V1). Evidence from brain imaging studies has shown visual functional network changes[22] and gray matter volume of occipital lobe[23] in diabetes without clinical retinopathy (NoDR). These results indicate that higher-level visual cortex areas beyond V1 may also be impaired in individuals with diabetes, both with and without retinopathy. However, it remains unclear whether there are any impairments in higher-level visual function in diabetes, especially in patients with diabetes without significant loss of visual acuity.

Second-order information, which is sensitive to variations in contrast and texture, is integrated within higher-order visual pathways (also known as the extrastriate cortex) including V2, V3, VP, V4, and middle-temporal.[24–26] It is as significant a component in the natural visual environment as first-order information (Fig. 1). Second-order visual function measurements could assist in assessing neural degeneration at the higher-level visual pathway. In addition, compared with retinal or brain imaging commonly used in clinics, visual functional measurements are more feasible and more cost-effective. Smartphone or tablet application comparative measurement makes it possible to test visual functions even outside the clinic. Therefore, the development of feasible and sensitive measurements for both vascular and neuronal deficits in the visual pathway is important for early screening and diabetic complications assessment.

Not only patients with DR but also NoDR, may have original neurovascular lesions in the retina, which can also affect visual function. To distinguish retinal abnormalities from cortical changes, the changes in the structure and function of the retina in DR need to be detected separately. Optical coherence tomography (OCT) and electroretinogram (ERG) are the most common methods used by researchers to detect early diabetic retinal changes. Many studies have detected retinal neurovascular structural changes in early DR by OCT and OCT angiography (OCTA), such as decreased vessel density, thinning of the retinal nerve fiber layer (RNFL), and disorganization of retinal inner layers (DRILs).[27–33] Some research suggests that multifocal ERG (mfERG) could be a more sensitive method for detecting the retinal neural dysfunction than a retinography and a delayed mfERG implicit time has been found to be a typical defect in patients with diabetes.[34–37]

Our study aimed to systematically find out visual deficits along the visual pathway and explore their correlation with retinal damages in patients with NoDR. Furthermore, we intended to assess which level of measurement is the most efficient for the early detection of diabetic visual function disorders within our scope of measurements. Thus, we measured visual function abnormalities of NoDR with normal visual acuity in this study by a novel battery of grayscale central visual psychophysical tests, which can identify impairments in both low- and high-order visual functions by utilizing both first-order and second-order stimuli. We also assessed retinal changes using OCT, OCTA, and mfERG to compare the accuracy of visual functional measurements with retinal tests in detecting visual disorders in patients with NoDR. The findings of our study have the potential to identify improved classifiers for the detection and evaluation of visual disorders in individuals with diabetes.

Methods

Participants

This research has received approval from the Ethics Committee of the First Affiliated Hospital of Anhui Medical University (PJ2022-09-48) and adhered to the tenets of the Declaration of Helsinki. All subjects were naive to the purpose of the psychophysical experiments, and their informed consent was obtained prior to their involvement.

This study included patients aged 18 to 65 years with T2DM[38] in the First Affiliated Hospital of Anhui Medical University in Heifei between December 2021 and September 2022. The eyes included the patients with NoDR group were required to meet the following inclusion criteria: no visible retinopathy (Early Treatment of Diabetic Retinopathy Study [ETDRS] score < 20, assessed through dilated fundal examination and non-mydriatic ultrawide field scanning laser ophthalmoscopy [Daytona, Optos, Dunfermline, UK])[39]; best corrected visual acuity (BCVA; specifically measured with ETDRS charts,[40] logarithm of the minimum angle of resolution [logMAR], 4-m test distance, subsequently denoted as ETDRS acuity) not exceeding 0.2 logMAR (Snellen equivalent = 20/32). Age-matched healthy controls (HCs) with normal vision in both eyes were recruited. The exclusion criteria for both patients and controls included cognitive impairment; the presence of significant lens opacities; high myopia; a history of glaucoma; ocular hypertension; or neuro-ophthalmic and brain disease. Capillary blood glucose levels of each participant were checked before visual psychophysical tests using a handheld glucose meter (ACCU-CHEK, USA) to ensure accuracy. Participants with T2DM should have capillary blood glucose levels not exceeding 10.0 mmol/L (180 mg/dL), whereas control participants should have capillary blood glucose levels not exceeding 7.5 mmol/L (135 mg/dL). Demographic and clinical information of patients with diabetes, including age, sex, duration of diabetes, hemoglobin $A1_C$ level ($HbA1_c$), body mass index (BMI), and hypoglycemic therapy were obtained from their most recent medical record within a 6-month period.

Visual Psychophysical Tests

Apparatus and Visual Stimuli

The stimuli were presented on a gamma-corrected 19-inch cathode ray tube monitor (Sony G220, Japan) with a mean luminance of 40 cd/m^2, a resolution of 1600 × 1200 pixels, and a refresh rate of 60 hertz (Hz). Using a custom-built device, the display system could produce 14-bit gray levels,[41] which enables contrast sensitivity measurement with a high precision. The stimuli were generated and controlled using Matlab software (the MathWorks, USA) and Psychophysics Toolboxes.[42,43] Four foveal tasks were used to evaluate grating acuity (subsequently denoted as GA), contrast sensitivity to first-order motion stimuli (1stM), contrast sensitivity to second-order stationary stimuli (2ndS), and contrast sensitivity to second-order motion stimuli (2ndM). All stimuli occupied 5.5 degrees of the visual angle, with the

blurred part occupying 0.5 degrees of the viewing angle. The first-order stimulus was a luminance-defined sine wave grating, whereas the second-order stimulus was a contrast-modulated sine wave grating with gray-scale noise carrier (Figs. 2A, 2B). The luminance profile at the point (x, y) of the first-order (Equation 1) and the second-order (Equation 2) stimuli[44] are defined as:

$$\boldsymbol{l}(\boldsymbol{x},\boldsymbol{y}) = \boldsymbol{L_m}\{1 + \boldsymbol{C}\cdot\sin\{2\pi[\boldsymbol{f}(y\cos\boldsymbol{\theta} - x\sin\boldsymbol{\theta}) + \boldsymbol{\omega}t] + \boldsymbol{\phi}\}\} \quad (1)$$

$$\boldsymbol{l}(\boldsymbol{x},\boldsymbol{y}) = \boldsymbol{L_m}\{1 + \boldsymbol{R}(\boldsymbol{x},\boldsymbol{y})\boldsymbol{C_c}\{1 + \boldsymbol{C}\cdot\sin[2\pi(\boldsymbol{f}(y\cos\boldsymbol{\theta} - x\sin\boldsymbol{\theta}) + \boldsymbol{\omega}t) + \boldsymbol{\phi}]\}\} \quad (2)$$

$\boldsymbol{L_m}$ is the display's background luminance; $\boldsymbol{C}$ is the grating contrast; $\boldsymbol{f}$ is the spatial frequency of the sine wave grating; $\boldsymbol{\theta}$ indicates the orientation of the grating (90 degrees in the motion direction discrimination task, or 45 degrees or 135 degrees in the orientation discrimination task); $\boldsymbol{\omega}$ is the temporal frequency of the moving grating (as ω is set to 0, the stimulus is static); $\boldsymbol{\phi}$ is the random initial spatial phase; and $\boldsymbol{R}(\boldsymbol{x}, \boldsymbol{y})$ is the static noise carrier, composed of single-pixel dots with values randomly assigned as 1 or −1; and $\boldsymbol{C_c}$ is the contrast of the noise carrier. The contrast of stimuli in the GA test was set to 1 and spatial frequency ranged from 3 to 36 cycles/degree. The spatial frequency of 2ndS was 1 cycle/degree. The spatial frequencies of 1stM and 2ndM gratings were 2 cycles/degree and the temporal frequencies were 4 cycles/second.

Experimental Design

The participant sat at a distance of 100.1 cm from the screen with one eye occluded in a dimly lit room. During the GA test, if the subjects were able to discern 14 cycles/degree or more, they were retested at a distance of 200.1 cm, and the stimuli were adjusted accordingly to maintain the same size in the visual angle. The participant's eyes were optimally corrected for visual acuity at the specific viewing distance. A chin-forehead-rest was used to minimize head movements during the experiment (Fig. 2C). A two-alternative-forced-choice paradigm and a weighted up-down adaptive method[44] were used. The inclusion of the GA and first-order tests served not only to assess first-order deficits but also to evaluate the suitability of the spatial frequency and contrast settings for the second-order test. Consequently, participants completed the tasks in the following order: GA, 1stM, 2ndS, and 2ndM. Each trial began with a brief beep, followed by the presentation of stimuli for 150 ms. Both the GA and 2ndS tasks involved stimulus orientation discrimination. Subjects were required to indicate the orientation of the stimulus by pressing the left or right key when it tilted 45 degrees to the left or right of the vertical. The 1stM and 2ndM tasks involved stimulus motion discrimination, with participants indicating the direction (leftward or rightward) by pressing the corresponding left or right key. The contrast of the stimuli was adjusted using a weighted up-down adaptive method. Correct responses resulted in an increase in task difficulty of 1.5 decibels (dB)/118.85% (decrease of image contrast or increase of spatial frequency depending on the task), whereas incorrect responses led to a decrease in task difficulty of 4.5 dB/167.88%. The procedure concludes when either 8 reversals are reached or a maximum of 80 trials are completed. No feedback regarding the correctness of the response was provided in the test sessions. Results were reported in terms of contrast threshold (the average end points in the adaptive procedure), the coefficient of variation of end points, and floor effect index (FEI; a value ranging from 0 to 1, with 1 indicating that stimulus contrast reached 1 or more in 20% of the trials, and 0 indicating that stimulus contrast never reached 1 in any of the trials). The contrast sensitivity (the inverse of the contrast threshold) was used for the analysis. If FEI was equal to 1 in a particular test, the contrast sensitivity was adjusted to 1. Each formal test session lasted 2 to 3 minutes. Prior to the start of the test sessions, each participant underwent a brief training session.

Retina Structural and Functional Tests

OCT Recording and Analysis

An RTVue OCT device was used (Avanti XR, version 2017; Optovue, Fremont, CA, USA), operating at an A-scan rate of 70,000 A-scans/s and providing 5-mm axial resolution. Each participant underwent a 3 mm × 3 mm macular OCTA scan, a peripapillary retinal nerve fiber layer (pRNFL) scan, and three ganglion cell complex (GCC) scans after full dilatation. All examinations were conducted by an experienced technician. The RTVue software version 6.12 automatically calculated the structural parameters of the fovea macula, pRNFL, and GCC (Figs. 3A–D). We categorized OCT information into two groups: vascular metrics (foveal avascular zone [FAZ] area, AI of FAZ, the foveal vascular density [FD-300, vessel density within 300 µm ring surrounding the FAZ], foveal vessel density in superficial capillary plexus [SCP] and deep capillary plexus [DCP], and the parafoveal vessel density in SCP and DCP); and thickness metrics (central macular thickness [CMT], GCC thickness, and temporal pRNFL thickness). Scans were excluded from the analysis if they had low signal strength, cropping artifacts, or failed segmentation.

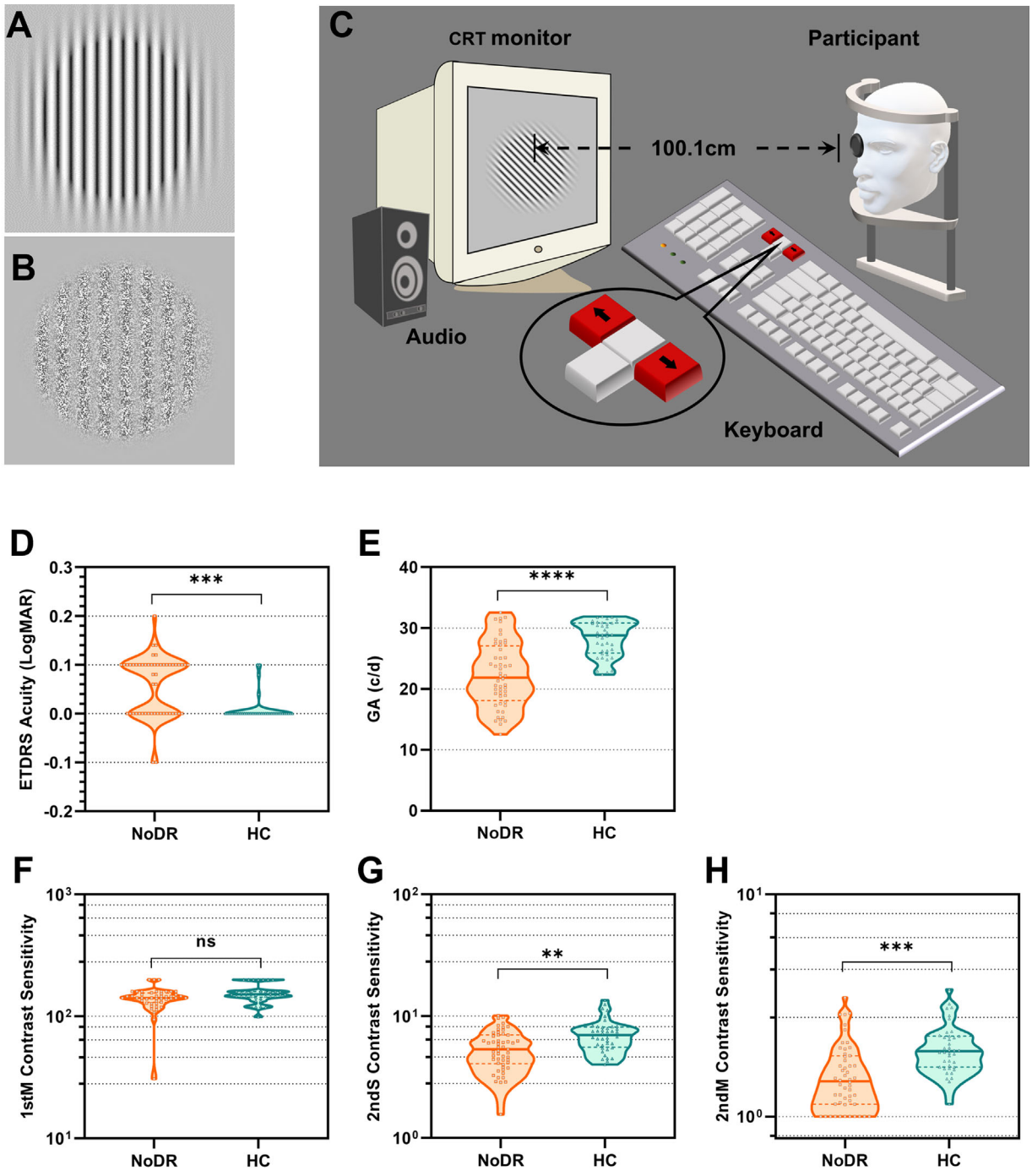

Figure 2. (**A**) Example visual stimuli of first-order grating. (**B**) Example visual stimuli of second-order grating. (**C**) Experimental design for psychophysical testing tasks. Comparison of multiple level of visual functions measured by psychophysical experiments in the NoDR group and the HC group shown are ETDRS acuity (**D**), GA (**E**), 1stM contrast sensitivity (**F**), 2ndS contrast sensitivity (**G**), and 2ndM contrast sensitivity (**H**). All points and median ± interquartile range in truncated violin plots are shown. Three lines in violin plots indicating quartile positions. *$P < 0.05$, **$P < 0.01$, ***$P < 0.001$, ****$P < 0.0001$ and ns = no significant difference. *P* values derived from this and the following group effect analysis were pooled together and adjusted to control FDR using Benjamini-Hochberg procedure. ETDRS, Early Treatment Diabetic Retinopathy Study; GA, grating acuity; 1stM, first-order motion stimulus; 2ndS, second-order stationary stimulus; 2ndM, second-order motion stimulus.

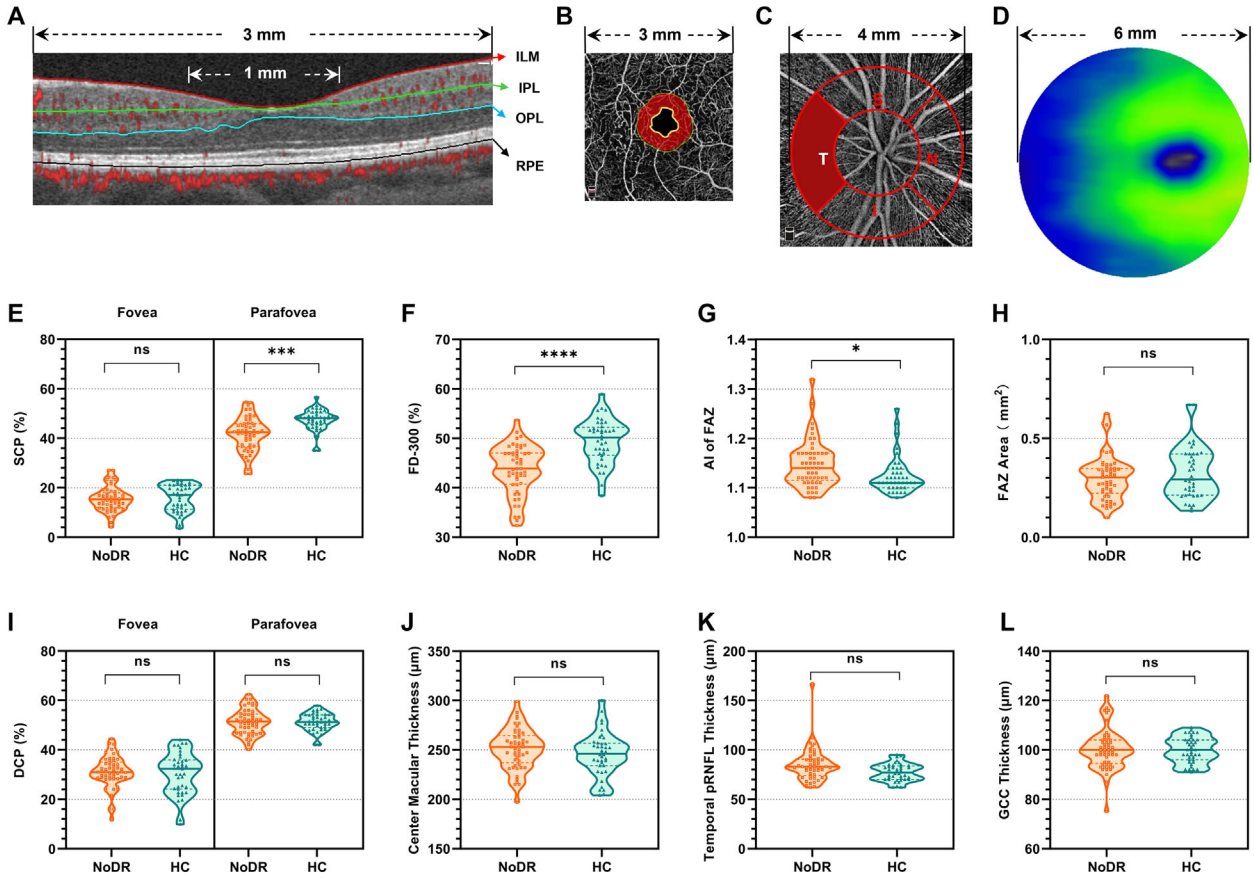

Figure 3. (**A**) Retina segmentation layers schematic in macular optical coherence tomography angiography scan. SCP, superficial capillary plexus; ILM, inner limiting membrane upper limit; IPL-10 µm, inner plexiform layer lower limit; DCP, deep capillary plexus; IPL-10 µm, upper limit; OPL+10 µm, lower limit; CMT, central macular thickness; ILM, upper limit; RPE, lower limit. The terms "foveal" and "parafoveal" were defined by the area of the center (1 mm) and the mean of the 4 quadrants of the area of the inner circle (1–3 mm) in the Early Treatment Diabetic Retinopathy Study (ETDRS) grid, respectively. (**B**) Macula central foveal measurements were based on 3 mm × 3 mm Angio retina scan and were generated based on the retina slab (ILM to OPL+10 µm). FAZ area is shaded in *black* and FD-300 is shaded in *red*. AI is the acircularity index-ratio between the measured FAZ perimeter and the perimeter of the same size circular area. (**C**) The parameter of pRNFL thickness was derived from a 2 to 4 mm diameter ring centered on the optic disc and the temporal quadrant (*shaded in red*, legend for right eye) was included in this study. (**D**) The GCC scan provided inner retinal thickness values from the ILM to the IPL. It was centered 1 mm temporal to the fovea in order to emphasize the temporal retina region within 6 mm width ring (accounting for 20 degrees of visual angle). Comparison of vascular metrics of the retina in the NoDR group and the HC group shown are foveal and parafoveal vessel density in SCP (**E**), FD-300 (**F**), AI of FAZ (**G**), FAZ area (**H**), and foveal and parafoveal vessel density in DCP (**I**). Comparison of thickness metrics of the retina in the NoDR group and the HC group shown are CMT (**J**), temporal pRNFL thickness (**K**), and GCC thickness (**L**). All points and median ± interquartile range in truncated violin plots are shown. Three lines in violin plots indicating quartile positions. *$P < 0.05$, **$P < 0.01$, ***$P < 0.001$, ****$P < 0.0001$ and ns = no significant difference. *P* values derived from this and the above group effect analysis were pooled together and adjusted to control for FDR using Benjamini-Hochberg procedure. AI, acircularity index; CMT, central macular thickness; DCP, deep capillary plexus; FAZ, foveal avascular zone; FD-300, vessel density within 300 µm ring surrounding the FAZ; GCC, ganglion cell complex; ILM, internal limiting membrane; IPL, inner plexiform layer; OPL, outer plexiform layer; pRNFL, peripapillary retinal nerve fiber layer; RPE, retinal pigment epithelium; SCP, superficial capillary plexus.

Any scan with a signal strength index below 6 was excluded.

mfERG Recording and Analysis

According to the International Society for Clinical Electrophysiology of Vision (ISCEV) standard,[45] mfERG recordings were obtained using the RETIport scan/21 (software version .3.11.1; Roland Consult, Germany) visual electrophysiology system and using a 103-hexagon strategy. The data obtained from the NoDR group were compared to a normative database consisting of 18 eyes from 18 age-matched HC

subjects in our facility. See the Supplementary Materials (mfERG Recording and Analysis) for more details.

Statistical Analysis

Statistical analyses were performed with IBM SPSS Statistics, version 23.0 (IBM Corp., Armonk, NY, USA) and MATLAB (R2014b; MathWorks, Inc.). Unless otherwise stated, means and SD were reported for continuous variables; numbers and percentages were reported for categorical variables. Two-sided $P < 0.05$ was considered significant. The contrast sensitivity in logarithmic units was used for statistical analysis. Before conducting any statistical tests, outliers in each variable were excluded following the 1.5 × interquartile range (IQR) rule. To eliminate an interocular correlation bias, generalized linear mixed effect (GLME) models were applied to analyze group effects and explore linear relationships between measurements. For the group effect analysis, each structural measurement or visual function served as the response variable, the group was regarded as the fixed effect, and the subject was considered the random effect, as follows: Visual Function or Structural Measurement ~ Group + (1|Subject). In the linear relationship analysis, each visual function was the response variable, the fixed effect consisted of the structural measurement and/or age and/or their interaction, and the subject was considered the random effect as follows: Visual Function ~ Structural Measurement + Age + (1|Subject), or Visual Function ~ Structural Measurement * Age + (1|Subject). Multiple comparisons were adjusted using the Benjamini-Hochberg procedure to control the false discovery rate (FDR).[46] Predicted probability of multiple combined indicators was calculated by the binary logistic regression model and was used in the receiver operating characteristic (ROC) analysis. The area under the ROC curve (AUC) was used to determine the optimal indicator for detecting visual deficits in patients with NoDR, and the AUC values were compared using DeLong's test. In order to avoid the possible influence of missing data in the statistics on the results, we again analyzed the data from only one eye included for each subject (33 patients with 33 eyes in the NoDR group and 27 HCs with 27 eyes were included). Based on the distribution of the data in each group, the differences between the groups were assessed with either *t*-test or Mann-Whitney test. Spearman correlation was used to assess the relationship between visual functions and other measurements (including age and retinal measurements) for patients with NoDR. We also used monocular data for ROC analyses.

Results

General Description

A total of 33 patients (26 men and 7 women) with 53 eyes in the NoDR group and 27 in the HC group (16 men and 11 women) with 40 eyes were included in this cross-sectional study. The mean ± SD age was 49.0 ± 9.5 years in the NoDR group, whereas in the control group, it was 48.0 ± 8.5 ($P = 0.396$). Members of the NoDR group had a median duration of diabetes of 8.0 years (IQR = 3.5–12.0 years), a median HbA_{1c} level of 8.6% (IQR = 6.80%–11.5%), and a median BMI of 22.49 kg/m^2 (IQR = 20.83–25.61 kg/m^2).

First- and Second-Order Visual Functional Deficits Were Found in the NoDR Group

Despite each participant having ETDRS acuity within the normal range, significant differences in visual functions were observed between the two groups. The NoDR group showed significant deficits in GA ($P < 0.0001$), as well as contrast sensitivity of 2ndS ($P = 0.003$) and 2ndM ($P = 0.0001$) compared with the HC group (Figs. 2E, 2G, 2H). To evaluate the ability of visual functional measurements in detecting diabetic dysfunctions, first, we calculated the proportion of abnormality, which represents the percentage of subjects whose visual function falls below the lower boundary of 95% confidence interval (CI) of that was observed in healthy subjects (Supplementary Table S1). In the NoDR group, the proportions of abnormalities were as follows: 76.9% (40/52 eyes) for GA, 61.7% (29/47 eyes) for 1stM, 56.6% (30/53 eyes) for 2ndS, and 71.2% (37/52 eyes) for 2ndM. Second, we calculated the proportion of subjects whose FEI was equal to one, indicating an almost complete inability to perform the task. We referred to this proportion as the "'proportion of floor effect'." For healthy subjects, the proportion of floor effect were 0% across all tasks. In the NoDR group, the proportions of floor effect were 0% in GA and 1stM, 1.89% in 2ndS (1/53 eye), and 13.21% in 2ndM (7/53 eyes). The results of the monocular data analysis were similar to the above results (see details in Supplementary Fig. S2).

Retinal Structural Changes in the NoDR Group

Retinal vascular parameters, including parafoveal SCP ($P = 0.0001$), FD-300 ($P < 0.0001$), and AI of FAZ ($P = 0.03$), significantly changed in the NoDR group compared with the HC group (Figs. 3E–G).

Table 1. Multivariate Generalized Linear Mixed Effect (GLME) Models to Predict Visual Functions

Response Variable	Adjusted R^2	Predictor Variable	Estimate	SE	95% CI	*P* Value*
1stM	0.27	Age	−0.0205	0.0056	(−0.0316 to −0.0094)	**0.0004**
		Parafoveal SCP	−0.0204	0.0062	(−0.0327 to −0.0080)	**0.0015**
		Parafoveal SCP* age	0.0005	0.0001	(0.0002 to 0.0007)	**0.0003**
		Intercept	3.0399	0.2746	(2.4928 to 3.5871)	**<0.0001**
2ndS	0.60	Age	−0.0062	0.0017	(−0.0097 to −0.0028)	**0.0005**
		Temporal pRNFL	−0.0038	0.0014	(−0.0066 to −0.0011)	**0.0067**
		Intercept	1.3933	0.1289	(1.1371 to 1.6496)	**<0.0001**

*No FDR correction was conducted here. Two-sided *P* values < 0.05 were regarded as significant. Statistically significant differences are highlighted in boldface.

No statistically significant differences were observed in retinal thickness parameters between the NoDR and the HC groups (all $P > 0.05$; Figs. 3J–L). For monocular data (Supplementary Fig. S3), there are still significant changes in parafoveal SCP ($P = 0.0018$) and FD-300 ($P < 0.0001$), but significant difference in temporal pRNFL thickness ($P = 0.023$) and marginal significant changes in AI of FAZ ($P = 0.077$).

Retinal Functional Changes in the NoDR Group

When compared with 18 eyes from 18 age-matched healthy control subjects (a new HC group, subsequently denoted as nHC group), the NoDR group exhibited only an increase (4.5%) in P1 implicit time of ring 2 (average was 46.53 ± 2.97 ms for the NoDR group and 44.32 ± 2.29 ms for the nHC group, $P = 0.004$; see Supplementary Fig. S1) in the mfERG test. No other significant differences were found between the NoDR group and the nHC group.

Factors Associated With Visual Function Changes

To explore the factors associated with visual function changes, we ran univariant GLME to assess the relationship between visual functions and other measurements, including age and retinal measurements, for all participants. Significant linear relationships were found between ETDRS acuity and age ($P = 0.02$); GA and age ($P = 0.04$), and 2ndS with age ($P = 0.006$), and with temporal pRNFL ($P = 0.04$) separately. Consistent with previous studies, age is associated with first- and second-order visual functions. No significance was found for the remaining visual functions. It should be noted that FDR was controlled using the Benjamini-Hochberg procedure for these analyses. Because there are two significant predictors for 2ndS in the univariant model, we included both predictors in the multivariate model to predict 2ndS. The results showed that temporal pRNFL and age remained significant predictors of 2ndS (adjusted $R^2 = 0.60$). To consider the impact of age and its potential interaction with other parameters in the correlation analysis, we constructed GLME models for each visual function using age, each respective parameter, and their interaction as predictors (Table 1). Our analysis revealed that age, parafoveal SCP, and their interaction were significant predictors of 1stM (adjusted $R^2 = 0.27$). However, no other significant relationship was observed for the remaining visual functions. Moreover, we computed Spearman correlation to assess the relationship between visual functions and other measurements (including age and retinal measurements) for NoDR using monocular data, and no significant relationship was observed between visual functions and other measurements. Significant relationships were found between ETDRS acuity and age ($r = 0.476$, $P = 0.005$); GA and age ($r = -0.465$, $P = 0.007$), and 2ndS with age ($r = -0.657$, $P < 0.0001$) separately (see details in Supplementary Fig. S4).

The Best Classifier for Detecting Diabetic Visual Disorders in Our Study

To determine whether grayscale central visual function or retinal structural tests measured by OCT and OCTA are more sensitive in detecting visual disorders in NoDR, we conducted ROC analyses using only monocular data (Table 2). The ROC curve for the top five classifiers in distinguishing diabetes from normal eyes are presented in Figure 4.

For detecting early diabetic visual disorders, the top five classifiers of those tests studied are GA (AUC = 0.829, 95% CI = 0.736 to 0.900, $P < 0.0001$), FD-300 (AUC = 0.822, 95% CI = 0.727 to 0.894, $P <$

Table 2. Classifying Performance of Visual Functional and Retinal Structural Parameters in Differentiating Patients With Diabetes From Healthy Patients

Parameter	AUC (95% CI)	Sensitivity, % (95% CI)	Specificity, % (95% CI)	*P* Value*
ETDRS acuity	0.751 (0.649 to 0.853)	60.8 (47.1 to 73.0)	92.5 (80.1 to 97.4)	**<0.0001**
GA	0.829 (0.745 to 0.914)	68.6 (55.0 to 79.7)	90.0 (77.0 to 96.0)	**<0.0001**
1stM	0.668 (0.551 to 0.784)	54.2 (40.3 to 67.4)	78.4 (62.8 to 88.6)	**0.0084**
2ndS	0.709 (0.605 to 0.813)	69.8 (56.5 to 80.5)	65.0 (49.5 to 77.9)	**0.0006**
2ndM	0.763 (0.665 to 0.861)	58.8 (45.2 to 71.3)	90.0 (77.0 to 96.0)	**<0.0001**
FAZ area	0.551 (0.429 to 0.673)	88.7(77.4 to 94.7)	35.0 (22.1 to 50.5)	0.4020
AI	0.670 (0.558 to 0.782)	54.7 (41.5 to 67.3)	75.0 (59.8 to 85.8)	**0.0052**
FD-300	0.822 (0.734 to 0.909)	94.1 (84.1 to 98.4)	60.0 (44.60 to 73.7)	**<0.0001**
Foveal SCP	0.543 (0.419 to 0.668)	69.8 (56.5 to 80.5)	55.0 (39.8 to 69.3)	0.4753
Foveal DCP	0.507 (0.383 to 0.632)	83.0 (70.8 to 90.8)	35.0 (22.1 to 50.5)	0.9073
Parafoveal SCP	0.785 (0.688 to 0.883)	62.8 (49.0 to 74.7)	92.5 (80.1 to 97.4)	**<0.0001**
Parafoveal DCP	0.509 (0.392 to 0.627)	30.2 (19.5 to 43.5)	87.5 (73.9 to 94.5)	0.8797
CMT	0.585 (0.467 to 0.702)	41.5 (29.3 to 54.9)	75.0 (59.8 to 85.8)	0.1625
Temporal pRNFL	0.655 (0.544 to 0.765)	35.9 (24.3 to 49.3)	90.0 (0.77.0 to 96.0)	**0.0110**
GCC	0.508 (0.389 to 0.627)	24.5 (14.9 to 37.6)	82.5 (68.1 to 91.3)	0.8950

*No FDR correction was conducted here. Two-sided *P* values < 0.05 were regarded as significant. Statistically significant differences are highlighted in boldface.

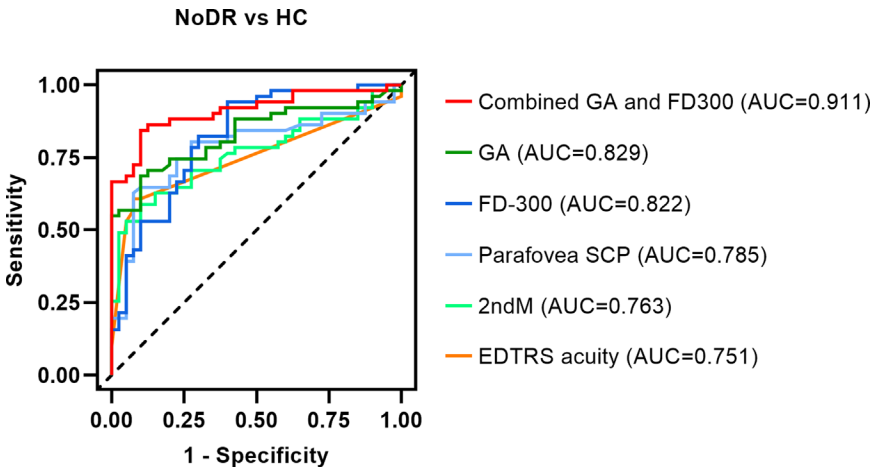

Figure 4. ROC curve for visual functions and retinal measurements in differentiating patients with diabetes from healthy patients.

0.0001), parafoveal SCP (AUC = 0.785, 95% CI = 0.686 to 0.864, $P < 0.0001$), 2ndM contrast sensitivity (AUC = 0.763, 95% CI = 0.662 to 0.846, $P < 0.0001$), and ETDRS acuity (AUC = 0.750, 95% CI = 0.649 to 0.835, $P < 0.0001$). Pairwise comparisons of ROC curves showed the classification ability of GA was similar to that of FD-300 ($P = 0.8985$). The cutoff point for GA to detect the diabetic visual dysfunction was less than 24.5 c/d (Youden index = 0.57) and the cutoff point for FD-300 was less than 48.9% (Youden index = 0.52). We calculated the positive predictive value (PPV) and negative predictive value (NPV) to further compare GA (PPV = 90.00% and NPV = 67.92%) and FD-300 (PPV = 75.38% and NPV = 85.71%). Moreover, the integration of GA and FD-300 (AUC = 0.911, 95% CI = 0.832 to 0.960, $P < 0.0001$, pairwise comparisons of ROC curves: all $P < 0.05$) can significantly improve detection performance (sensitivity = 84.31%, specificity = 90.0%, PPV = 91.67%, and NPV = 80.00%).

The results of the ROC analysis using only monocular data are similar (Supplementary Fig. S5). For the monocular data, the top five classifiers of those tests studied are GA (AUC = 0.822, 95% CI = 0.713 to 0.931, $P < 0.0001$), FD-300 (AUC = 0.814, 95% CI = 0.700 to 0.927, $P < 0.0001$), 2ndM contrast sensitivity

(AUC = 0.779, 95% CI = 0.663 to 0.895, $P = 0.0002$), parafoveal SCP (AUC = 0.742, 95% CI = 0.613 to 0.872, $P = 0.0013$), and ETDRS acuity (AUC = 0.736, 95% CI = 0.607 to 0.864, $P < 0.0018$).

Discussion

In this study, we found significantly reduced low-level and higher-level visual functions in patients with diabetes with NoDR. Specifically, we noted significant declines in grating acuity, contrast sensitivity for second-order stationary stimuli (2ndS), and contrast sensitivity for motion stimuli (2ndM). OCTA detected microvascular changes in AI of FAZ, FD-300, and parafoveal SCP before the emergence of visible microaneurysms in the diabetic retina. We further demonstrated that compared with OCT measurements, visual function measurements have similar or superior classification ability for diabetes. Combining sophisticated visual functional measurements and retinal microvascular tests could provide accurate and effective assessments for detecting early diabetic visual disorders.

Neurophysiological studies have uncovered distinct mechanisms for processing first-order and second-order visual information in the cortex.[47–50] Higher-level visual function deficits have been found in glaucoma,[51] amblyopia,[52] and age-related degeneration.[44,53] However, the impact of diabetes on higher-level visual function, including cases without retinopathy, has not been previously documented. In our study, we found no significant impairment in 1stM but a reduction in 2ndM for NoDR. The proportion of abnormality and the occurrence of a floor effect were notably higher for 2ndM task compared to the 1stM task for NoDR. The NoDR group also demonstrated impairments in discriminating second-order stationary stimuli with contrast modulation. Besides, the spatial and temporal parameters we set for second-order stimuli are far below the threshold of first-order test, which means that all participants are able to recognize the first-order visual information in the second-order task. Processing first-order information in the second-order test was not the bottleneck for both groups. Thus, our findings suggest that the reduced contrast sensitivity observed in the second-order task is likely a result of difficulties in integrating second-order visual information rather than a deficit in processing first-order information.

Numerous studies have confirmed that retinal microvascular changes could be present before the clinically visible lesions in diabetes.[30–33] We also found a significant decrease in the retinal vascular parameter FD-300 and the parafoveal SCP in NoDR, serving as metrics reflecting the capillary loss in the parafoveal area. Meanwhile, our results showed significantly increased AI of FAZ but no significant change of FAZ area. This suggests that the distortion of the FAZ edge may precede the enlargement of the FAZ area in adults with diabetes without retinopathy, a pattern also observed in children with type 1 diabetes.[54] Some studies have also suggested that FAZ acircularity can have higher sensitivity and lower inter-person variability compared to the FAZ area.[55–57] ROC analysis suggests that FD-300 may be a relatively more sensitive indicator of macular perfusion impairment than the other retinal metrics, aligning with previous research findings.[58] Additionally, the delayed P1 implicit time we found in this study suggests the presence of bipolar cell abnormalities in the retina and some other studies found it may also be an early indicator of capillary closure.[59] Compared with the HCs, the other diabetes-related retinal alterations in NoDR are relatively minor at this stage in our study. This is partly attributed to included patients having more stable blood glucose levels and better visual acuity in this study. On the other hand, some subtle diabetic retinal changes might not be detectable through OCT or OCTA but could be identified using advanced retinal imaging methods techniques, such as adaptive optics OCT and adaptive optics scanning laser ophthalmoscopy.[60–62]

The GLME models showed temporal pRNFL might be one of the predictors of 2ndS and parafoveal SCP might be correlated with 1stM. However, it would be insufficiently justified to attribute visual dysfunctions to retinal changes alone. This is because no statistically significant differences in temporal pRNFL and 1stM between the two groups were found in GLME analysis. In particular, the decline in 2ndM was not significantly associated with retinal changes despite some visual functions correlating with these retinal changes. Tang et al. also found no obvious relationship between impaired low-order visual function and retinal structural changes in patients with early DR.[63] It implies that there may also be some neurological damage to the central nervous system in patients with early diabetes mellitus. These findings are in agreement with brain imaging results that have detected changes in the visual network[22] and the gray matter volume of the occipital lobe[23] in patients with diabetes without retinopathy. The study by Cunha-Vaz et al. suggests that some individuals with diabetes could manifest deficits vascularly rather than neurally at first,[64] which could be another reason for not finding significant correlation between the retinal vascular changes and higher-order visual function changes. Additional research is warranted to identify the origin

of the visual functional deficits observed in patients with NoDR and to investigate the potential benefits of neuroprotective supplements and more frequent follow-up examinations could be useful for those with higher-order visual deficit.

Some researchers have found that visual functions, such as contrast sensitivity and color vision, in patients with diabetes are related to $HbA1_c$ levels.[65,66] To test whether the changes in visual functions are related with $HbA1_c$, in this study, we performed regression analysis only for the NoDR group. We did not find significant correlations between $HbA1_c$ and visual functions. This could be attributed to the fact that the $HbA1_c$ values were extracted from the patients' most recent medical records, which were not measured concurrently with the visual function assessments. Another reason for lack of correlation could be because the fact that the $HbA1_c$ has too limited a range in this sample. Subsequent studies, incorporating blood tests conducted simultaneously with visual function assessments, may help elucidate the relationship between changes in visual function and the severity of diabetes.

The deficits in both retina structure and visual functions of T2DM may be related to alterations in the NVU, as the NVU determines the ability of the retina and brain to adapt to changes in local microcirculation and metabolism, and may be directly impaired by T2DM. Particularly, active brain regions require more oxygen and nutrients than other regions and are more susceptible to disturbances in glucose metabolism. The NVU in the brains of patients with T2DM, dysregulation of insulin signaling in neurons, astrocytes, and endothelial cells were presented, as shown in a transcriptome study.[67] Moreover, it has been shown that disruption of neurovascular coupling in high-level brain regions occurs early in T2DM by functional magnetic resonance imaging (fMRI).[68] Furthermore, multiple studies have indicated that T2DM is associated with an elevated risk of cognitive impairment and dementia,[69–71] implying susceptibility of high-order cortical areas to T2DM. Further research studies are needed to explore potential mechanisms underlying impaired high-level visual function in individuals with diabetes.

The ROC analysis further found that grating acuity and FD-300 almost equally distinguish the patients with NoDR from the HCs. Grating acuity exhibited a higher positive predictive value, whereas FD-300 demonstrated a superior negative predictive value. Integrating these two measurements provided a more precise classification. These findings indicate that integrating visual functional and retinal structure measurements could enhance the early detection of visual disorder in NoDR. It should be noted that due to the ceiling effect shown in GA measurements, the AUC of GA may be underestimated. Improved experiment settings may help increase the classification ability of GA. The high AUC for 2ndM suggests that higher-level visual deficits should not be ignored in patients with NoDR. The majority of studies have exclusively relied on chart-based visual acuity to assess vision loss in patients with diabetes, which may be inadequate in detecting the extent of early visual deficits. Grating acuity more effectively captured early mild visual acuity dysfunction than ETDRS acuity in patients with diabetes. Therefore, we suggest that it is necessary to apply more sophisticated visual functional measurements to widespread clinical practices.

Our findings suggest that these novel visual functional measurements, which can be readily integrated into a cell phone or computer interface, hold promise as a potential tool for early diabetes detection. Furthermore, in addition to the tests used in this study, color vision tests and peripheral tests are extensively used in clinical practice and can identify abnormalities that arise before clinically evident DR develops.[14–20] More convenient examination methods pertaining to color vision and visual fields could also be developed and compared with GA in future studies. Moreover, combining noninvasive visual function measurements and retinal imaging tests can lead to higher detection accuracy.

This study had several limitations. First, this study was cross-sectional and could not provide continuous information about visual function changes and their relationship with other diabetic changes. Subsequent studies with longitudinal designs and larger sample sizes can be conducted to explore whether visual functional deficits are early signs of developing DR or other neuronal complexions. Second, certain visual functions in our study reached either the floor effect or ceiling effect due to the limitations of the selected stimuli parameters. Fine-tuning these parameters can enhance the accuracy of classification. We can increase the spatial frequency range in the GA test by adjusting the test distance and can reduce the spatial frequency of the second-order test to reduce the difficulty of the test in future studies. Third, due to limitations in resources and time, it was not feasible to include all pertinent visual functional tests. In this study, our primary objective was to examine higher-order visual deficits, especially pertaining to second-order information processing in patients with NoDR. Hence, we focused on utilizing our current battery of tests and did not compare color or peripheral tests with our novel battery of visual psychophysical tests. Nevertheless, it would be valuable to compare sensitive tests, such as color tests and peripheral tests, in future studies

for the purpose of diabetes screening. Future studies combining retinal and brain imaging technology could help to address this question. Finally, this study only focused on foveal and parafoveal vascular variables, which are insufficient for good prediction, but slightly larger regions of interest may produce better results.

In this study, we found notable deficits in both low- and higher-order visual functions for patients with NoDR with normal visual acuity, and these deficits seem to be not significantly correlated with retinal thickness or vascular changes. Grating acuity and FD-300 appeared to be the most sensitive measurements for detecting early visual disorders associated with diabetes within the scope of our study. The combination of retinal imaging tests and advanced visual function measurements could lead to a comprehensive evaluation of the visual system's status concerning diabetes.

Acknowledgments

The authors thank Lun Liu, Jianyang Gong, and Jie Zheng for their assistance during recruiting the subjects for this study. The authors also thank the participants who were involved in this study.

Supported by the Natural Science Foundation of China Grant NSFC 82371094 (LF), National Science and Technology Innovation 2030 Major Program Grant 2022ZD0210000 (RL) Anhui Province's Key Research and Development Plan Grant 202004j07020038 (LF), Natural Science Foundation of China Grant NSFC 82201230 (RL), and CAS Project for Young Scientists in Basic Research Grant YSBR-041 (RL), and National Science and Technology Innovation 2030 Major Program Grant 2022ZD0204800 (RL).

Disclosure: **S. Luo**, None; **L. Xia**, None; **Y. Wang**, None; **Y. Tang**, None; **J. Dong**, None; **R. Liu**, None; **L. Feng**, None

References

1. Sun H, Saeedi P, Karuranga S, et al. IDF Diabetes Atlas: global, regional and country-level diabetes prevalence estimates for 2021 and projections for 2045. *Diabetes Res Clin Pr*. 2022;183:109119.
2. Magliano DJ, Boyko EJ, IDF Diabetes Atlas 10th Edition Scientific Committee. *IDF Diabetes Atlas*. 10th ed. Brussels, Belgium: International Diabetes Federation; 2021.
3. Yang S, Zhang J, Chen L. The cells involved in the pathological process of diabetic retinopathy. *Biomed Pharmacother*. 2020;132:110818.
4. Little K, Llorián-Salvador M, Scullion S, et al. Common pathways in dementia and diabetic retinopathy: understanding the mechanisms of diabetes-related cognitive decline. *Trends Endocrinol Metab*. 2022;33(1):50–71.
5. Abcouwer SF, Gardner TW. Diabetic retinopathy: loss of neuroretinal adaptation to the diabetic metabolic environment. *Ann N Y Acad Sci*. 2014;1311:174–190.
6. Santos AR, Ribeiro L, Bandello F, et al. Functional and structural findings of neurodegeneration in early stages of diabetic retinopathy: cross-sectional analyses of baseline data of the EUROCONDOR project. *Diabetes*. 2017;66(9):2503–2510.
7. Simó R, Hernández C; European Consortium for the Early Treatment of Diabetic Retinopathy (EUROCONDOR). Neurodegeneration in the diabetic eye: new insights and therapeutic perspectives. *Trends Endocrinol Metab*. 2014;25(1):23–33.
8. Layton CJ, Safa R, Osborne NN. Oscillatory potentials and the b-wave: partial masking and interdependence in dark adaptation and diabetes in the rat. *Graefes Arch Clin Exp Ophthalmol*. 2007;245(9):1335–1345.
9. Eggers ED. Visual Dysfunction in Diabetes. *Annu Rev Vis Sci*. 2023;9:91–109.
10. Solomon SD, Chew E, Duh EJ, et al. Diabetic retinopathy: a position statement by the American Diabetes Association. *Diabetes Care*. 2017;40:412–418.
11. Cusick M, Sangiovanni JP, Chew EY, et al. Central visual function and the NEI-VFQ-25 near and distance activities subscale scores in people with type 1 and 2 diabetes. *Am J Ophthalmol*. 2005;139(6):1042–1050.
12. Pramanik S, Chowdhury S, Ganguly U, Banerjee A, Bhattacharya B, Mondal LK. Visual contrast sensitivity could be an early marker of diabetic retinopathy. *Heliyon*. 2020;6(10):e05336.
13. Silva-Viguera MC, García-Romera MC, Bautista-Llamas MJ. Contrast sensitivity function under three light conditions in patients with type 1 diabetes mellitus without retinopathy: a cross-sectional, case-control study. *Graefes Arch Clin Exp Ophthalmol*. 2023;261(9):2497–2505.
14. Zico OA, El-Shazly AA-F, Ahmed EEA-H. Short wavelength automated perimetry can detect visual

field changes in diabetic patients without retinopathy. *Indian J Ophthalmol*. 2014;62(4):383–387
15. Bao YK, Yan Y, Gordon M, McGill JB, Kass M, Rajagopal R. Visual field loss in patients with diabetes in the absence of clinically-detectable vascular retinopathy in a nationally representative survey. *Invest Ophthalmol Vis Sci*. 2019;60(14):4711–4716.
16. McAnany JJ, Park JC, Lim JI. Visual field abnormalities in early-stage diabetic retinopathy assessed by chromatic perimetry. *Invest Ophthalmol Vis Sci*. 2023;64(2):8.
17. Feitosa-Santana C, Paramei GV, Nishi M, Gualtieri M, Costa MF, Ventura DF. Color vision impairment in type 2 diabetes assessed by the D-15d test and the Cambridge Colour Test. *Ophthal Physl Opt*. 2010;30(5):717–723.
18. Shoji T, Sakurai Y, Sato H, Chihara E, Takeuchi M. Do type 2 diabetes patients without diabetic retinopathy or subjects with impaired fasting glucose have impaired colour vision? The Okubo Color Study Report. *Diabet Med*. 2011; 28(7): 865–871.
19. Tan NC, Yip WF, Kallakuri S, Sankari U, Koh YLE. Factors associated with impaired color vision without retinopathy amongst people with type 2 diabetes mellitus: a cross-sectional study. *BMC Endocr Disord*. 2017; 17(1): 29.
20. Tsai LT, Chen CC, Hou CH, Liao KM. Achromatic and chromatic contrast discrimination in patients with type 2 diabetes. *Sci Rep*. 2023;13(1):7420.
21. Chen H, Wang M, Xia L, et al. New evidence of central nervous system damage in diabetes: impairment of fine visual discrimination. *Diabetes*. 2022;71(8):1772–1784.
22. Zhang D, Huang Y, Gao J, et al. Altered functional topological organization in type-2 diabetes mellitus with and without microvascular complications. *Front Neurosci-switz*. 2021;15:726350.
23. Ferreira FS, Pereira JMS, Reis A, et al. Early visual cortical structural changes in diabetic patients without diabetic retinopathy. *Graefes Arch Clin Exp Ophthalmol*. 2017;255(11):2113–2118.
24. Bussières L, Casanova C. Neural processing of second-order motion in the suprasylvian cortex of the cat. *Cereb Cortex*. 2017;27(2):1347–1357.
25. Li G, Yao Z, Wang Z, et al. Form-cue invariant second-order neuronal responses to contrast modulation in primate area V2. *J Neurosci*. 2014;34(36):12081–12092.
26. Smith AT, Greenlee MW, Singh KD, Kraemer FM, Hennig J. The processing of first- and second-order motion in human visual cortex assessed by functional magnetic resonance imaging (fMRI). *J Neurosci*. 1998;18(10):3816–3830.
27. Joltikov KA, Sesi CA, de Castro VM, et al. Disorganization of retinal inner layers (DRIL) and neuroretinal dysfunction in early diabetic retinopathy. *Invest Ophthalmol Vis Sci*. 2018;59(13):5481–5486.
28. Lee MW, Lee WH, Ryu CK, Lee YM, Lee YH, Kim JY. Peripapillary retinal nerve fiber layer and microvasculature in prolonged type 2 diabetes patients without clinical diabetic retinopathy. *Invest Ophthalmol Vis Sci*. 2021;62(2):9.
29. Chai Q, Yao Y, Guo C, Lu H, Ma J. Structural and functional retinal changes in patients with type 2 diabetes without diabetic retinopathy. *Ann Med*. 2022;54(1):1816–1825.
30. Kim K, Kim ES, Yu SY. Optical coherence tomography angiography analysis of foveal microvascular changes and inner retinal layer thinning in patients with diabetes. *Br J Ophthalmol*. 2018;102(9):1226–1231.
31. Zhang B, Chou Y, Zhao X, Yang J, Chen Y. Early detection of microvascular impairments with optical coherence tomography angiography in diabetic patients without clinical retinopathy: a meta-analysis. *Am J Ophthalmol*. 2021;222:226–237.
32. Dimitrova G, Chihara E, Takahashi H, Amano H, Okazaki K. Quantitative retinal optical coherence tomography angiography in patients with diabetes without diabetic retinopathy. *Invest Ophthalmol Vis Sci*. 2017;58(1):190–196.
33. Li B, Li W, Guo C, Guo C, Chen M. Early diagnosis of retinal neurovascular injury in diabetic patients without retinopathy by quantitative analysis of OCT and OCTA. *Acta Diabetol*. 2023;60(8):1063–1074.
34. Srinivasan S, Sivaprasad, S, Rajalakshmi R, et al. Retinal structure-function correlation in type 2 diabetes. *Eye (Lond)*. 2022;36(10):1865–1871.
35. McAnany JJ, Persidina OS, Park JC. Clinical electroretinography in diabetic retinopathy: a review. *Surv Ophthalmol*. 2022;67(3):712–722.
36. Bearse MA, Jr, Adams AJ, Han Y, et al. A multifocal electroretinogram model predicting the development of diabetic retinopathy. *Prog Retin Eye Res*. 2006;25(5):425–448.
37. Bronson-Castain KW, Bearse MA, Jr, Neuville J, et al. Adolescents with type 2 diabetes: early indications of focal retinal neuropathy, retinal thinning, and venular dilation. *Retina*. 2009;29(5):618–626.
38. ElSayed NA, Aleppo G, Aroda VR, et al. 2. Classification and diagnosis of diabetes: standards of care in diabetes—2023. *Diabetes Care*. 2023;46(Supplement_1):S19–S40.

39. Early Treatment Diabetic Retinopathy Study Research Group. Grading diabetic retinopathy from stereoscopic color fundus photographs — an extension of the modified Airlie House Classification: ETDRS Report Number 10. *Ophthalmology*. 2020;127(4):S99–S119.
40. Ferris FL, Kassoff A, Bresnick GH, Bailey I. New visual acuity charts for clinical research. *Am J Ophthalmol*. 1982;94(1):91–96.
41. Li X, Lu ZL, Xu P, Jin J, Zhou Y. Generating high gray-level resolution monochrome displays with conventional computer graphics cards and color monitors. *J Neurosci Meth*. 2003;130(1):9–18.
42. Brainard DH. The Psychophysics Toolbox. *Spat Vis*. 1997;10(4):433–436.
43. Pelli DG. The VideoToolbox software for visual psychophysics: transforming numbers into movies. *Spat Vis*. 1997;10(4):437–442.
44. Tang Y, Zhou Y. Age-related decline of contrast sensitivity for second-order stimuli: Earlier onset, but slower progression, than for first-order stimuli. *J Vision*. 2009;9(7):18.
45. Hoffmann MB, Bach M, Kondo M, et al. ISCEV standard for clinical multifocal electroretinography (mfERG) (2021 update). *Doc Ophthalmol*. 2021 Feb;142(1):5–16.
46. Groppe DM, Urbach TP, Kutas M. Mass univariate analysis of event-related brain potentials/fields I: a critical tutorial review. *Psychophysiology*. 2011;48(12):1711–1725.
47. Ashida H, Lingnau A, Wall MB, Smith AT. FMRI adaptation reveals separate mechanisms for first-order and second-order motion. *J Neurophysiol*. 2007;97(2):1319–1325.
48. Duarte JV, Pereira JM, Quendera B, et al. Early disrupted neurovascular coupling and changed event level hemodynamic response function in type 2 diabetes: an fMRI study. *J Cereb Blood Flow Metab*. 2015;35(10):1671–1680.
49. Vaina LM, Cowey A, Kennedy D. Perception of first- and second-order motion: separable neurological mechanisms? *Hum Brain Mapp*. 1999;7(1):67–77.
50. Smith AT, Greenlee MW, Singh KD, Kraemer FM, Hennig J. The processing of first- and second-order motion in human visual cortex assessed by functional magnetic resonance imaging (fMRI). *J Neurosci*. 1998;18(10):3816–3830.
51. Hirji SH, Hood DC, Liebmann JM, Blumberg DM. Association of patterns of glaucomatous macular damage with contrast sensitivity and facial recognition in patients with glaucoma. *JAMA Ophthalmol*. 2021;139(1):27–32.
52. Aaen-Stockdale C, Ledgeway T, Hess RF. Second-order optic flow deficits in amblyopia. *Invest Ophthalmol Vis Sci*. 2007;48(12):5532.
53. Reynaud A, Tang Y, Zhou Y, Hess RF. Second-order visual sensitivity in the aging population. *Aging Clin Exp Res*. 2019;31(5):705–716.
54. Inanc M, Tekin K, Kiziltoprak H, Ozalkak S, Doguizi S, Aycan Z. Changes in retinal microcirculation precede the clinical onset of diabetic retinopathy in children with type 1 diabetes mellitus. *Am J Ophthalmol*. 2019;207:37–44.
55. Waheed NK, Rosen RB, Jia Y, et al. Optical coherence tomography angiography in diabetic retinopathy. *Prog Retin Eye Res*. 2023;97:101206.
56. Linderman RE, Muthiah MN, Omoba SB, et al. Variability of foveal avascular zone metrics derived from optical coherence tomography angiography images. *Trans Vis Sci Tech*. 2018;7(5):20.
57. Ashraf M, Nesper PL, Jampol LM, Yu F, Fawzi AA. Statistical model of optical coherence tomography angiography parameters that correlate with severity of diabetic retinopathy. *Invest Ophthalmol Vis Sci*. 2018;59(10):4292–4298.
58. Li X, Xie J, Zhang L, et al. Identifying microvascular and neural parameters related to the severity of diabetic retinopathy using optical coherence tomography angiography. *Invest Ophthalmol Vis Sci*. 2020;61(5):39.
59. Srinivasan S, Sivaprasad S, Rajalakshmi R, et al. Assessment of optical coherence tomography angiography and multifocal electroretinography in eyes with and without nonproliferative diabetic retinopathy. *Indian J Ophthalmol*. 2021;69(11):3235–3240.
60. Kreis J, Carroll J. Applications of adaptive optics imaging for studying conditions affecting the fovea. *Annu Rev Vis Sci*. 2024;10(1):239–262.
61. Kurokawa K, Nemeth M. Multifunctional adaptive optics optical coherence tomography allows cellular scale reflectometry, polarimetry, and angiography in the living human eye. *Biomed Opt Express*. 2024;15(2):1331–1354.
62. Song H, Hang H, Li K, Rossi EA, Zhang J. Longitudinal adaptive optics scanning laser ophthalmoscopy reveals regional variation in cone and rod photoreceptor loss in Stargardt disease. *Retina*. 2024;44(8):1403–1412.
63. Tang VTS, Symons RCA, Fourlanos S, Guest D, McKendrick AM. The relationship between ON-OFF function and OCT structural and angiographic parameters in early diabetic retinal disease. *Ophthalmic Physiol Opt*. 2025;45(1):77–88.

64. Cunha-Vaz J, Ribeiro L, Lobo C. Phenotypes and biomarkers of diabetic retinopathy. *Prog Retin Eye Res*. 2014;41:90–111.
65. Shah M, Farooq A, Tariq Y. Relationship between glycosylated hemoglobin levels and contrast sensitivity in people with type 2 diabetes mellitus without diabetic retinopathy. *Turk J Ophthalmol*. 2022;52(6):394–399.
66. Karson N, Smith J, Jones M, Datta A, Richdale K, Harrison WW. Functional retinal outcomes in patients with prediabetes and type 2 diabetes. *Ophthalmic Physiol Opt*. 2020;40(6):770–777.
67. Bury JJ, Chambers A, Heath PR, et al. Type 2 diabetes mellitus-associated transcriptome alterations in cortical neurones and associated neurovascular unit cells in the ageing brain. *Acta Neuropathol Commun*. 2021;9(1):5
68. Duarte JV, Pereira JM, Quendera B, et al. Early disrupted neurovascular coupling and changed event level hemodynamic response function in type 2 diabetes: an fMRI study. *J Cereb Blood Flow Metab*. 2015;35(10):1671–1680.
69. Ding X, Yin L, Zhang L, et al. Diabetes accelerates Alzheimer's disease progression in the first year post mild cognitive impairment diagnosis. *Alzheimers Dement*. 2024;20(7):4583–4593.
70. Lee CS, Krakauer C, Su YR, et al. Diabetic retinopathy and dementia association, beyond diabetes severity. *Am J Ophthalmol*. 2023;249:90–98.
71. Little K, Llorián-Salvador M, Scullion S, et al. Common pathways in dementia and diabetic retinopathy: understanding the mechanisms of diabetes-related cognitive decline. *Trends Endocrinol Metab*. 2022;33(1):50–71.